

## Supporting Information

# Tuning the Conduction Band for Interfacial Electron Transfer: Dye-Sensitized $\text{Sn}_x\text{Ti}_{1-x}\text{O}_2$ Photoanodes for Water Splitting

Jacob A. Spies\*, John R. Swierk†, H. Ray Kelly, Matt D. Capobianco, Kevin P. Regan, Victor S. Batista, Gary W. Brudvig, Charles A. Schmuttenmaer§

Department of Chemistry and Energy Sciences Institute, Yale University, New Haven, CT 06520  
United States

\*Corresponding Author E-Mail: jacob.spies@aya.yale.edu

†Current Address: Department of Chemistry, State University of New York at Binghamton, Binghamton, NY 13902

§Deceased: July 26<sup>th</sup>, 2020

## Table of Contents

<b>Supplemental Materials Characterization .....</b>	S3
<i>Near-Infrared (NIR) Spectroelectrochemistry and Tauc Measurements .....</i>	S3
<b>Figure S1.....</b>	S3
<b>Figure S2.....</b>	S3
<b>Figure S3.....</b>	S4
<b>Figure S4.....</b>	S4
<i>X-Ray Photoelectron Spectroscopy Measurements.....</i>	S5
<b>Figure S5.....</b>	S5
<b>Figure S6.....</b>	S6
<i>Transmission Electron Microscopy.....</i>	S6
<b>Figure S7.....</b>	S6
<i>Powder X-Ray Diffraction Measurements .....</i>	S7
<b>Figure S8.....</b>	S7
<i>UV-Vis and X-Ray Absorption Spectroscopy .....</i>	S8
<b>Figure S9.....</b>	S8
<b>Figure S10.....</b>	S8
<i>Periodic Density Functional Theory Calculations.....</i>	S9
<b>Figure S11.....</b>	S9
<b>Figure S12.....</b>	S9
<i>Ultrafast Transient Absorption Spectroscopy.....</i>	S10

<b>Figure S13</b> .....	S10
<b>Figure S14</b> .....	S10
<b>Materials Characterization Data Tables</b> .....	S11
<b>Table S1</b> .....	S11
<b>Table S2</b> .....	S11
<b>Table S3</b> .....	S11
<b>Table S4</b> .....	S12
<b>Table S5</b> .....	S12
<b>Table S6</b> .....	S12
<b>Table S7</b> .....	S13
<b>Table S8</b> .....	S13
<b>Table S9</b> .....	S13
<b>Table S10</b> .....	S14
<b>Table S11</b> .....	S14
<b>Table S12</b> .....	S14
<b>Table S13</b> .....	S15
<b>Table S14</b> .....	S16
<b>Table S15</b> .....	S16
<b>Table S16</b> .....	S17
<b>Table S17</b> .....	S17
<b>Table S18</b> .....	S18
<b>Table S19</b> .....	S19
<b>Table S20</b> .....	S20
<b>References</b> .....	S23

## Supplemental Materials Characterization

As mentioned in the main text, two separate  $\text{SnO}_2$  pastes were prepared using small ( $\sim 5 \text{ nm}$ ), synthesized<sup>1</sup> particles ( $\text{SnO}_2\text{-S}$ ) and larger ( $\sim 22\text{-}43 \text{ nm}$ ), commercial particles ( $\text{SnO}_2\text{-L}$ ). Herein, the notation  $\text{SnO}_2\text{-S}$  and  $\text{SnO}_2\text{-L}$  for “Small” and “Large,” respectively, will be used to differentiate these two samples. Notably, there were no differences in IET behavior (Figure S10 and Table S1) or parameters extracted from PXRD measurements (Table S11 and Table S12).  $\text{SnO}_2\text{-L}$  was chosen for NIR spectroelectrochemistry and Tauc measurements because the film was thicker and more uniform than  $\text{SnO}_2\text{-S}$  (see Table S5), which resulted in higher, more reliable signal in NIR spectroelectrochemistry and Tauc measurements.

### Near-Infrared (NIR) Spectroelectrochemistry and Tauc Measurements

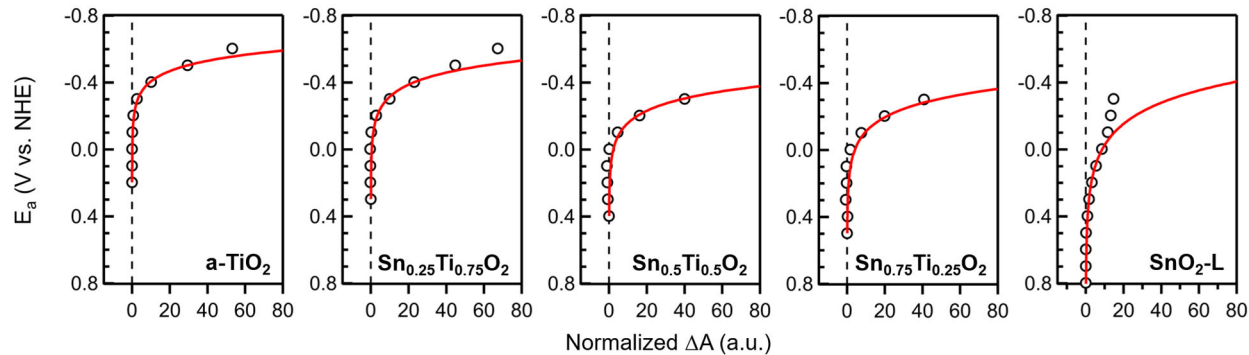


**Figure S1.** Normalized NIR spectroelectrochemistry measurements of RuP-sensitized  $\text{Sn}_x\text{Ti}_{1-x}\text{O}_2$  in 0.1 M  $\text{HClO}_4$  to determine the conduction band minimum ( $E_{CBM}$ ) of  $\text{Sn}_x\text{Ti}_{1-x}\text{O}_2$ , showing  $E_{CBM}$  shift to more oxidizing potentials as the Sn content increases. Data points (black circles) represent the change in absorbance at 800 nm relative to the most positive applied potential ( $E_a$ ) and were fit to Equation 4 in the main text. The data plotted above were normalized on the amplitude extracted from the fit in Equation 4 (see  $\Delta A_0$  in Table S2).

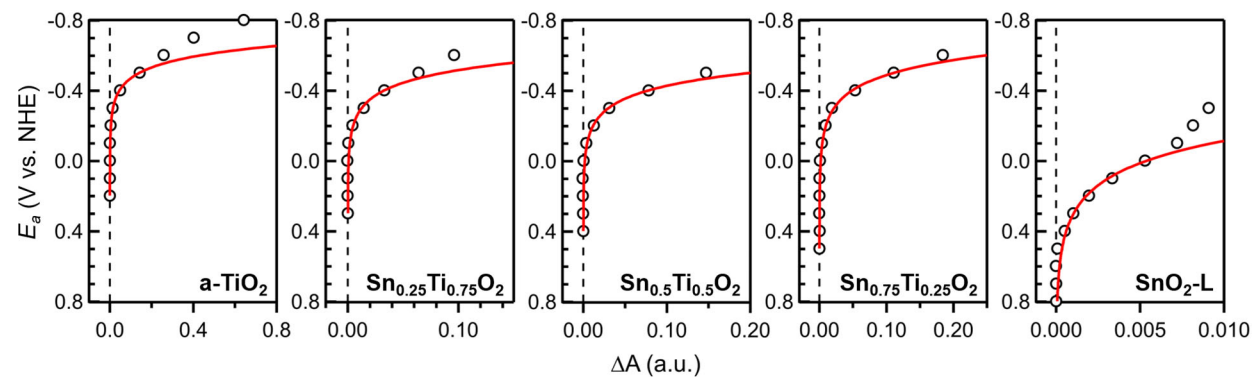


**Figure S2.** Raw NIR spectroelectrochemistry measurements of  $\text{Sn}_x\text{Ti}_{1-x}\text{O}_2$  showing all of the data points collected without normalization. Data points (black circles) are the change in absorbance at 800 nm relative to the most positive applied potential ( $E_a$ ) and were fit to Equation 4 in the main text (red line).

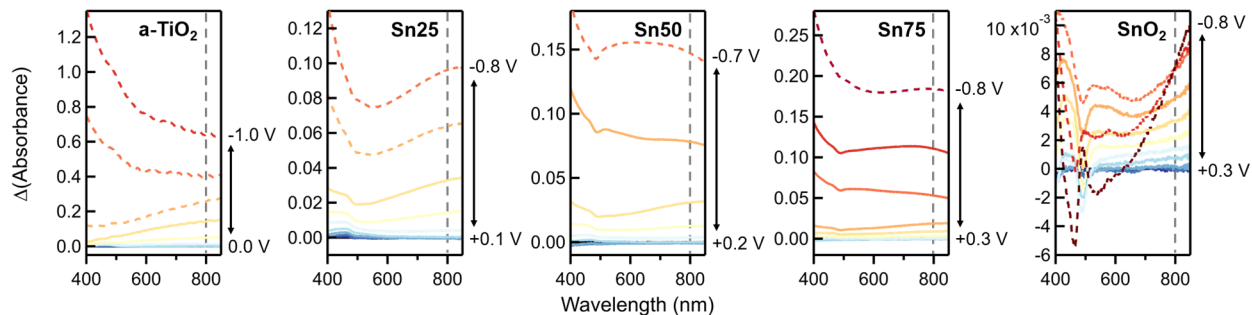


**Figure S3.** Optical absorption spectra of RuP-sensitized  $\text{Sn}_x\text{Ti}_{1-x}\text{O}_2$  in 0.1 M  $\text{HClO}_4$  (pH 1) collected for NIR spectroelectrochemical measurements. Spectra are plotted as difference spectra relative to the most positive potential in each dataset. Potential ranges are reported on the right side of each plot as they were measured in V vs. Ag/AgCl (can be converted to NHE by adding 0.197 V).<sup>2</sup> The potential steps between each spectra in each series was 0.1 V. Spectra plotted as dashed lines were excluded from the fit to determine  $E_{CBM}$  shown in Figure S1-2 due to deviations from exponential behavior (which only holds close to the band edge) or sample degradation (e.g., burning at high reducing potentials). A gray dashed line is included at 800 nm, where data points were taken to determine  $E_{CBM}$ .

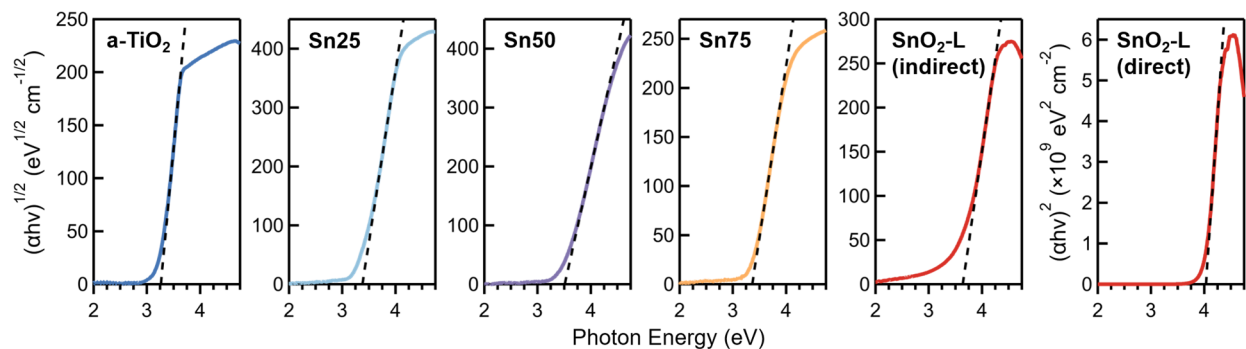


**Figure S4.** Tauc plots and linear fits to extract the bandgap ( $E_G$ ) of  $\text{Sn}_x\text{Ti}_{1-x}\text{O}_2$  measured using a Shimadzu UV-2600 with an ISR-2600Plus integrating sphere accessory as described in the main text. The extracted bandgaps are tabulated in Table S3 below.

*X-Ray Photoelectron Spectroscopy Measurements*

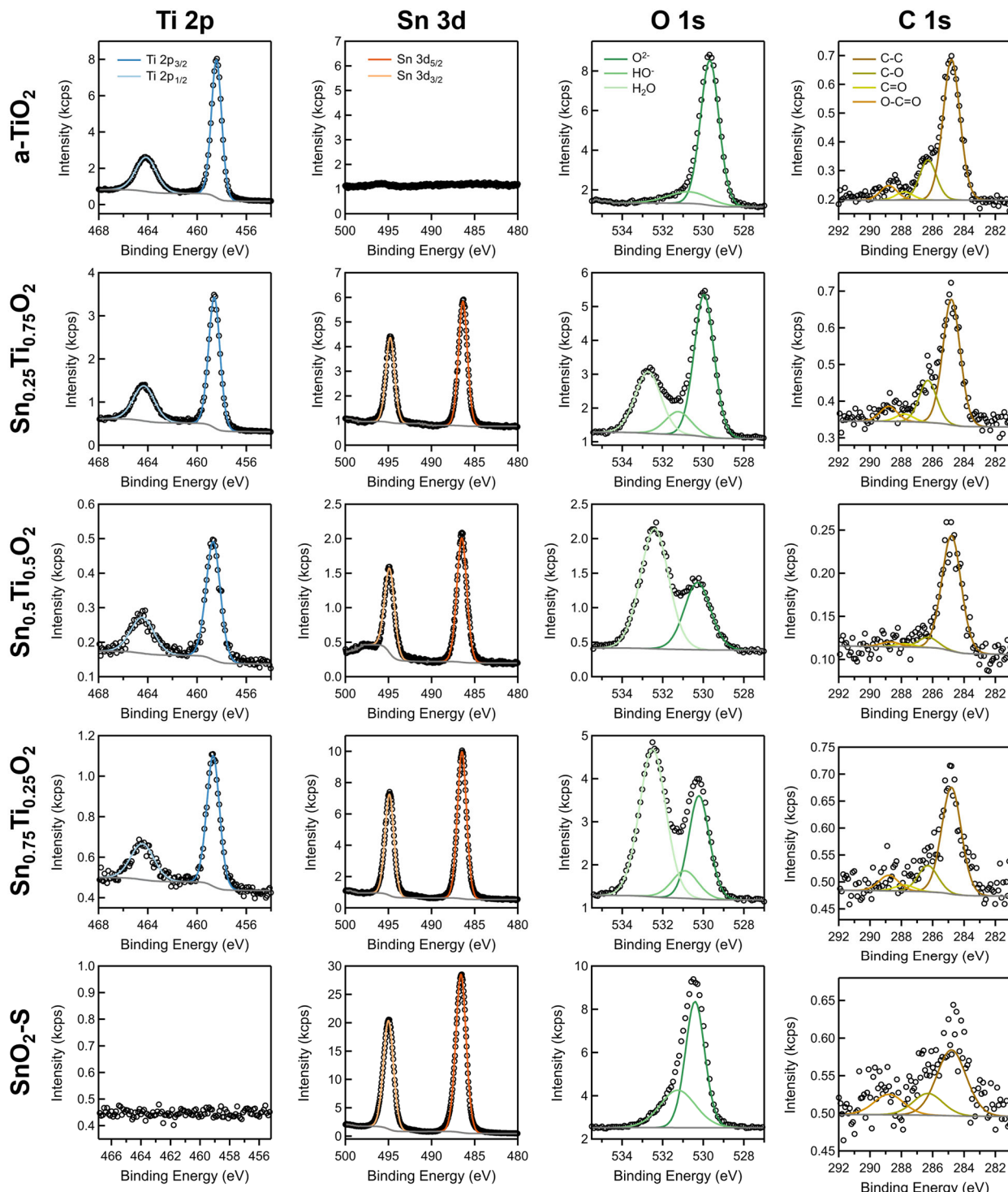


**Figure S5.** High-resolution XPS measurements of  $\text{Sn}_x\text{Ti}_{1-x}\text{O}_2$  in the Ti 2p, Sn 3d, O 1s, and C 1s regions. Spectra were charged corrected to the main adventitious carbon peak in the C 1s region, assuming a binding energy of 284.8 eV.<sup>3</sup> Data were fit in CasaXPS using the GL(30) peak function and the resulting fits are shown in Tables S13-S16.

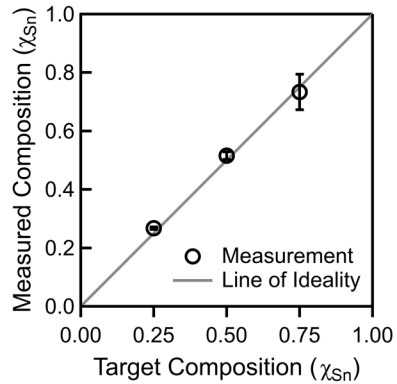


**Figure S6.** Relative composition for  $\text{Sn}_{0.25}\text{Ti}_{0.75}\text{O}_2$  (Sn25),  $\text{Sn}_{0.5}\text{Ti}_{0.5}\text{O}_2$  (Sn50), and  $\text{Sn}_{0.75}\text{Ti}_{0.25}\text{O}_2$  (Sn75) as determined by XPS vs. the stoichiometric ratio used in the synthesis. The compositions were calculated using relative sensitivity factor (RSF) values calculated relative to the oxide and hydroxide peaks in the O 1s region for the pure metal oxides ( $\text{TiO}_2$  and  $\text{SnO}_2$ ) assuming a 1:2 stoichiometric ratio of metal to oxide. Using both commercial and synthesized samples, RSF values of  $2.3 \pm 0.1$  and  $12.8 \pm 0.3$  were determined for Ti and Sn, respectively. Errors represent the standard deviation of the average of multiple samples.

#### Transmission Electron Microscopy

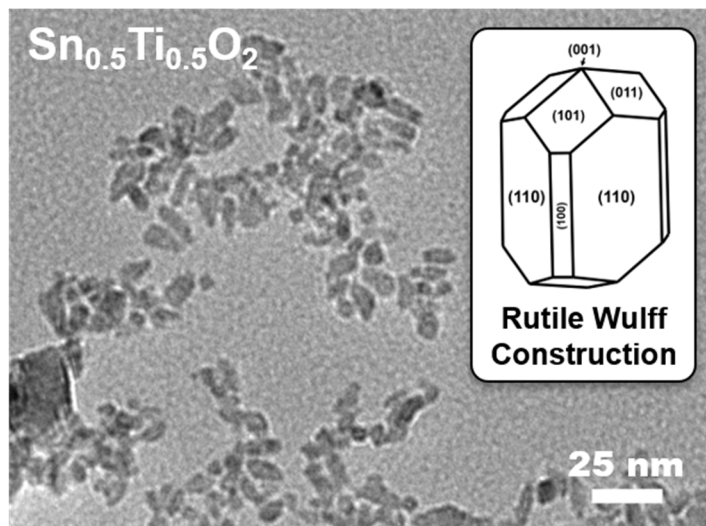


**Figure S7.** TEM micrograph of  $\text{Sn}_{0.5}\text{Ti}_{0.5}\text{O}_2$ , showing that particles are ca. 5 nm in size, consistent with PXRD, and appear to have a growth pattern consistent with the rutile Wulff construction (see inset, adapted and redrawn from Ref. 4).

### Powder X-Ray Diffraction Measurements

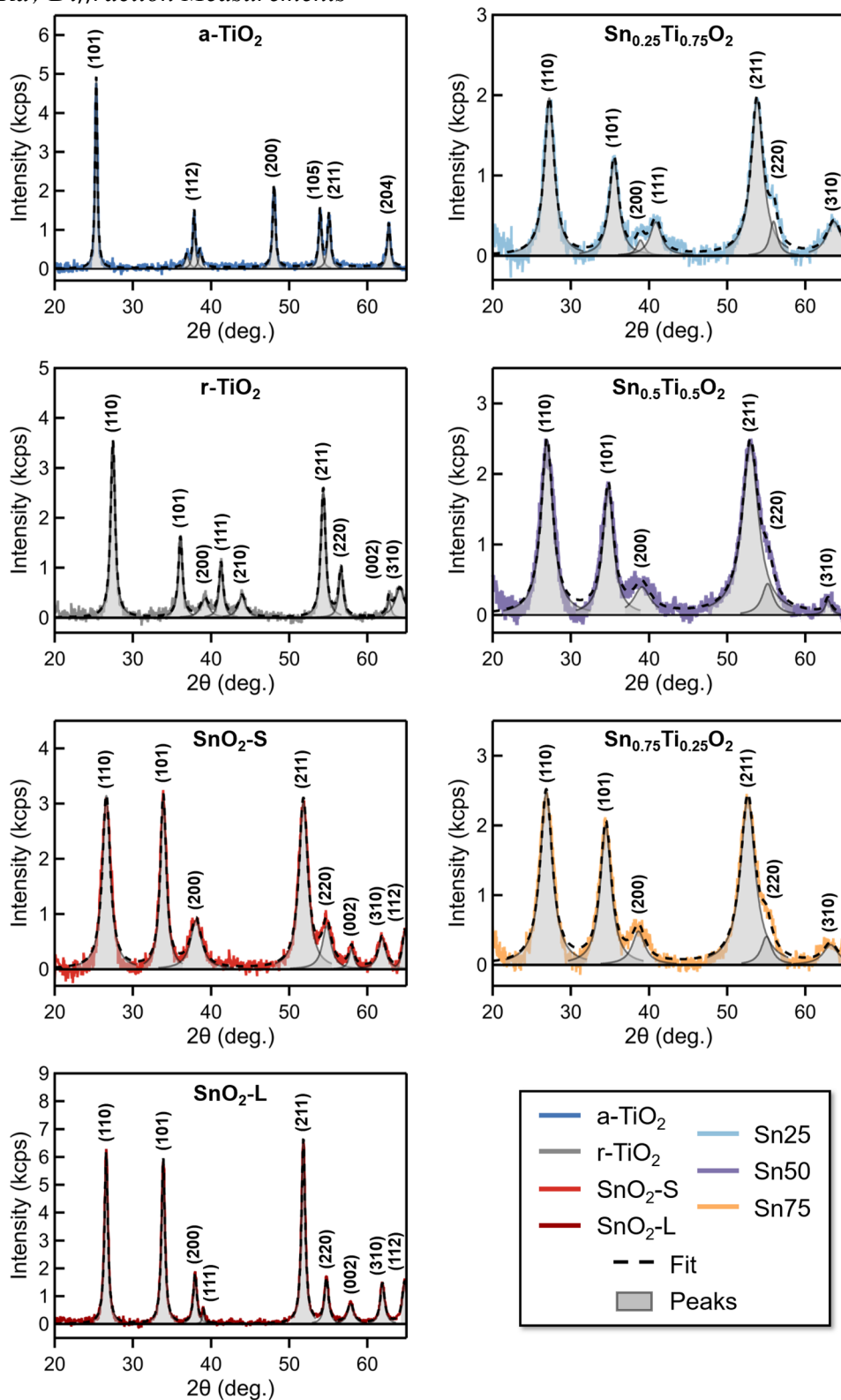


**Figure S8.** PXRD patterns of  $\text{Sn}_x\text{Ti}_{1-x}\text{O}_2$  fit to a sum of Lorentzian functions. The resulting fit parameters are shown in Tables S6-S12.

*UV-Vis and X-Ray Absorption Spectroscopy*

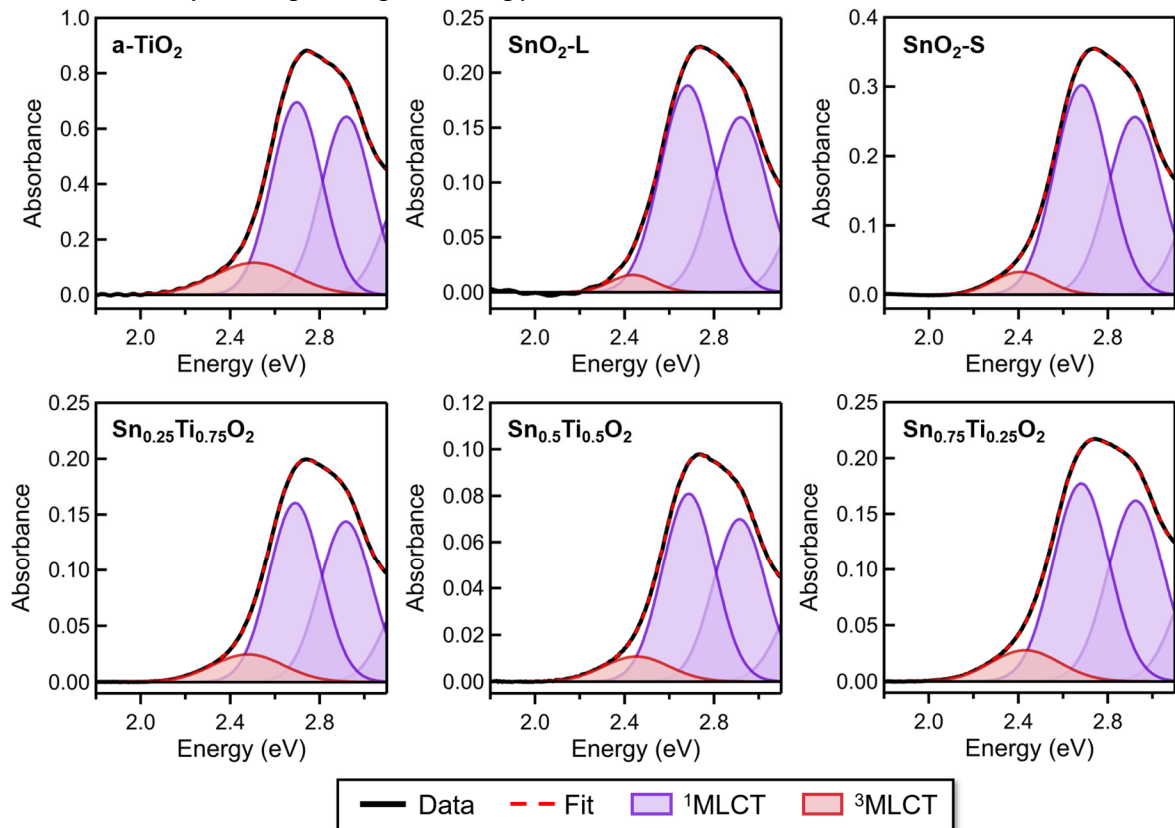


**Figure S9.** Representative spectra of dry RuP-sensitized  $\text{Sn}_x\text{Ti}_{1-x}\text{O}_2$  fit to a sum of Gaussians to compare the relative multiplicity fraction as a function of composition (see Figure 4 and Table S18). Spectra were also used to determine dye loadings as shown below in Table S5.

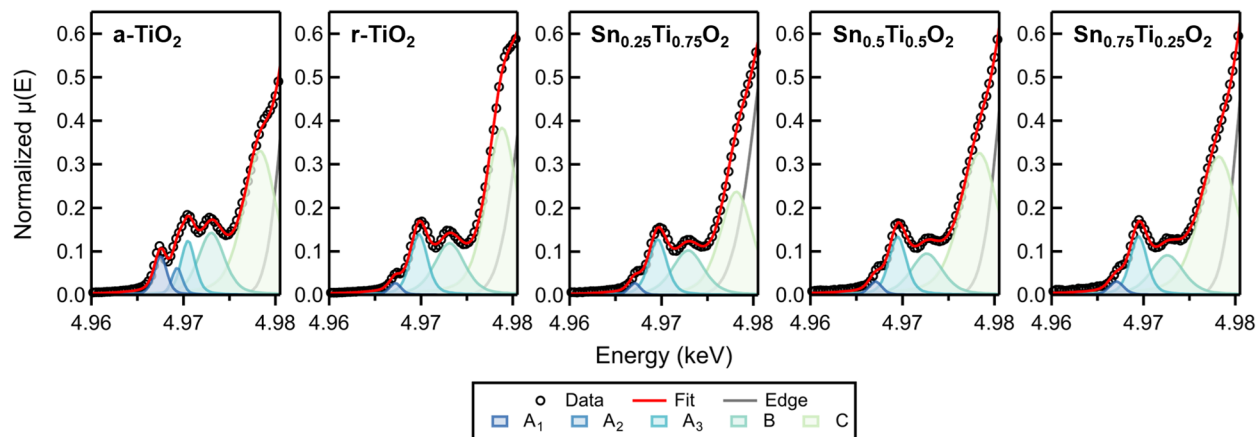


**Figure S10.** Fits of pre-edge X-ray absorption spectra at the Ti K-edge of  $\text{Sn}_x\text{Ti}_{1-x}\text{O}_2$ . Data were fit using the Athena XAS data processing software, part of the Demeter package.<sup>5</sup> Fit parameters are shown in Table S17.

*Periodic Density Functional Theory Calculations*

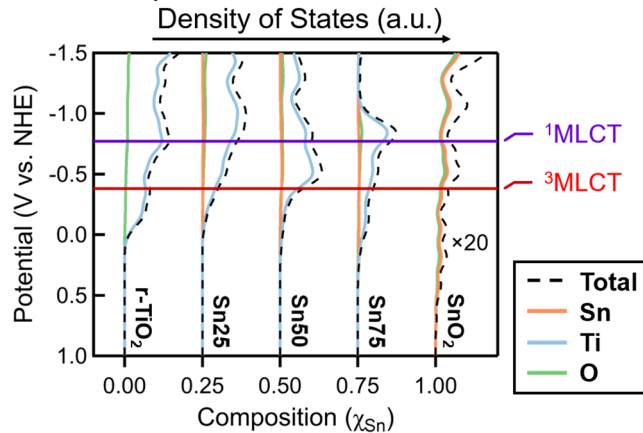


**Figure S11.** Conduction band density of states (DOS) for  $\text{Sn}_x\text{Ti}_{1-x}\text{O}_2$  calculated using periodic DFT, with rutile  $\text{TiO}_2$  ( $\text{r-TiO}_2$ ) included instead of anatase  $\text{TiO}_2$  ( $\text{a-TiO}_2$ ). Partial DOS for Ti, Sn, and O are shown in blue, orange, and green solid lines, respectively. The total DOS is shown as a dashed black line. Excited states potentials of RuP are included for reference.

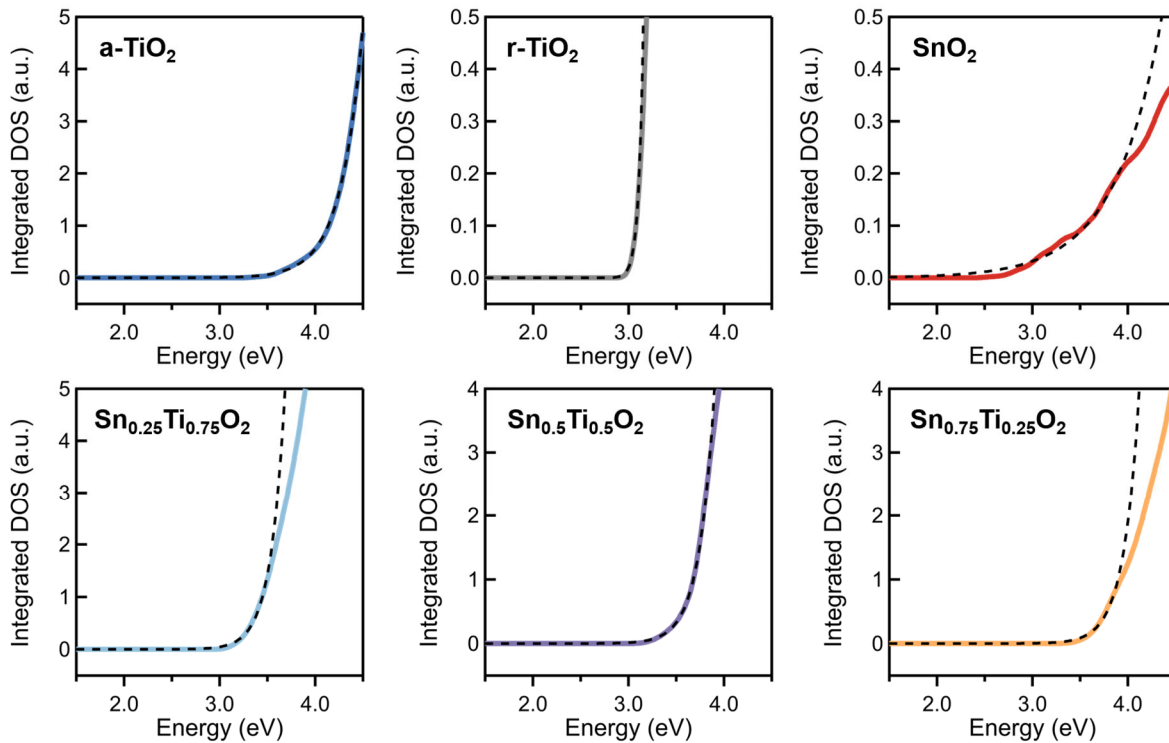


**Figure S12.** Integrated density of states (DOS) near the band edge calculated using periodic DFT. The data are shown in solid-colored lines and the fits to Equation 4 in the main text are shown in dashed black lines. The fit results are shown in Table S4 and were used to correct  $E_{CBM}$  values to match the experimental values in Figure 5a in the main text and Figure S7 above.

*Ultrafast Transient Absorption Spectroscopy*

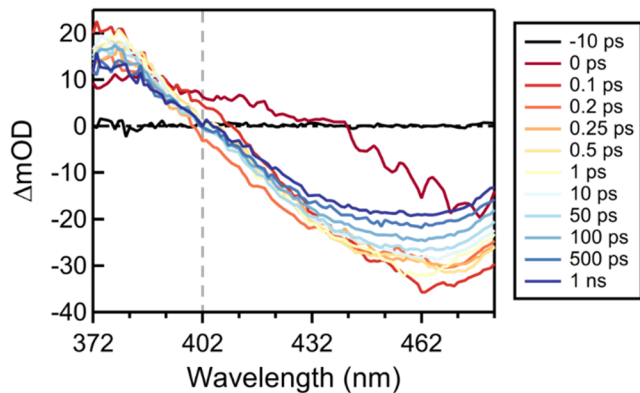


**Figure S13.** RuP-sensitized ZrO<sub>2</sub> fs-TAS measurements to determine the RuP<sup>2+</sup> ground-excited state isosbestic point (occurs at 402 nm, denoted by a gray dashed line). Samples were photoexcited at 515 nm and probed using a white light continuum generated in CaF<sub>2</sub>. The dye loading on ZrO<sub>2</sub> was  $(3.1 \pm 0.4) \times 10^{-8}$  mol cm<sup>-2</sup> as determined by UV-Vis spectroscopy as previously described.<sup>6,7</sup>

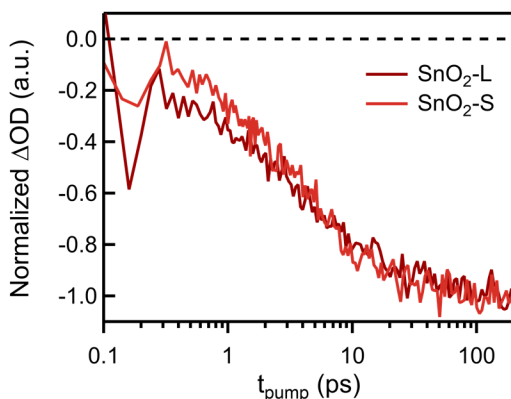


**Figure S14.** Comparison of representation fs-TAS traces for small, synthesized (SnO<sub>2</sub>-S) and larger, commercial (SnO<sub>2</sub>-L) RuP-sensitized SnO<sub>2</sub> dynamics measured by fs-TAS, illustrating similarity of IET character shown to be within error in Table S1.

## Materials Characterization Data Tables

**Table S1.** Fit parameters obtained from fs-TAS measurements. Errors are reported as the standard deviation of the average of four independently measured samples, except where otherwise noted.

	$A_1$	$A_3$	$\tau_3$ (ps)	$\beta$	$\langle \tau_3 \rangle^b$ (ps)	Scaling (mOD)
a-TiO <sub>2</sub>	$0.2 \pm 0.1$	$0.8 \pm 0.1$	$8 \pm 2$	$0.5 \pm 0.1$	$17 \pm 10$	$8 \pm 3$
Sn <sub>0.25</sub> Ti <sub>0.75</sub> O <sub>2</sub>	$0.4 \pm 0.1$	$0.6 \pm 0.1$	$4 \pm 1$	$0.76 \pm 0.05$	$5 \pm 2$	$3 \pm 2$
Sn <sub>0.5</sub> Ti <sub>0.5</sub> O <sub>2</sub>	$0.52 \pm 0.07$	$0.48 \pm 0.07$	$5 \pm 1$	$0.7 \pm 0.2$	$6 \pm 3$	$1.7 \pm 0.9$
Sn <sub>0.75</sub> Ti <sub>0.25</sub> O <sub>2</sub>	$0.66 \pm 0.02$	$0.34 \pm 0.02$	$10 \pm 2$	$0.8 \pm 0.2$	$11 \pm 3$	$1.1 \pm 0.4$
SnO <sub>2</sub> -S	$0.04 \pm 0.09$	$0.96 \pm 0.09$	$6 \pm 3$	$0.6 \pm 0.1$	$9 \pm 4$	$1.8 \pm 1.0$
SnO <sub>2</sub> -L	$0.03 \pm 0.05$	$0.97 \pm 0.05$	$5 \pm 2$	$0.53 \pm 0.09$	$8 \pm 4$	$3.1 \pm 0.8$

<sup>b</sup> Errors are propagated using the experimental errors in  $\tau_3$  and  $\beta$ .

**Table S2.** Fit parameters from fits in Figure S1 to Equation 4 to determine the conduction band minimum ( $E_{CBM}$ ) of Sn<sub>x</sub>Ti<sub>1-x</sub>O<sub>2</sub> samples. Errors represent the uncertainty in the fit.

Sample	$E_{CBM}$ (V vs. NHE)	$\Delta A_0 (\times 10^{-3}$ a.u.)	$a$ (unitless)
a-TiO <sub>2</sub>	$-0.2029 \pm 0.0010$	$4.84 \pm 0.05$	$0.29 \pm 0.05$
Sn <sub>0.25</sub> Ti <sub>0.75</sub> O <sub>2</sub>	$-0.076 \pm 0.003$	$1.43 \pm 0.04$	$0.2 \pm 0.1$
Sn <sub>0.5</sub> Ti <sub>0.5</sub> O <sub>2</sub>	$0.085 \pm 0.001$	$0.775 \pm 0.010$	$0.24 \pm 0.02$
Sn <sub>0.75</sub> Ti <sub>0.25</sub> O <sub>2</sub>	$0.171 \pm 0.002$	$0.456 \pm 0.006$	$0.211 \pm 0.010$
SnO <sub>2</sub> -L	$0.392 \pm 0.005$	$0.62 \pm 0.02$	$0.14 \pm 0.01$

**Table S3.** Bandgaps ( $E_G$ ) of Sn<sub>x</sub>Ti<sub>1-x</sub>O<sub>2</sub> extracted using Tauc analysis of films measured using an integrating sphere and valence band maximum ( $E_{VBM}$ ) determined by subtracting  $E_G$  from  $E_{CBM}$ . Indirect allowed bandgaps were assumed, unless other noted. Errors represent uncertainty determined by propagation of error.

Sample	$E_G$ (eV)	$E_{VBM}$ (V vs. NHE)
a-TiO <sub>2</sub>	$3.26 \pm 0.01$	$3.06 \pm 0.01$
Sn <sub>0.25</sub> Ti <sub>0.75</sub> O <sub>2</sub>	$3.38 \pm 0.02$	$3.30 \pm 0.02$
Sn <sub>0.5</sub> Ti <sub>0.5</sub> O <sub>2</sub>	$3.51 \pm 0.01$	$3.60 \pm 0.01$
Sn <sub>0.75</sub> Ti <sub>0.25</sub> O <sub>2</sub>	$3.364 \pm 0.007$	$3.535 \pm 0.008$
SnO <sub>2</sub> -L (direct)	$4.03 \pm 0.04$	$4.42 \pm 0.04$
SnO <sub>2</sub> -L (indirect)	$3.641 \pm 0.006$	$4.033 \pm 0.008$

**Table S4.** Fit parameters for the fits in Figure S12 to Equation 4 to determine correction factors to shift the calculated DOS in Figure 5a and Figure S11 to correspond with the experimental  $E_{CBM}$  values shown above in Table S2.

Sample	$E_{CBM}$ (eV)	$\Delta A_\theta (\times 10^{-3} \text{ a.u.})$	$a$ (unitless)
a-TiO <sub>2</sub>	$3.5260 \pm 0.0002$	$0.0719 \pm 0.0005$	$0.1118 \pm 0.0002$
r-TiO <sub>2</sub>	$3.0631 \pm 0.0002$	$0.0740 \pm 0.0004$	$0.537 \pm 0.005$
Sn <sub>0.25</sub> Ti <sub>0.75</sub> O <sub>2</sub>	$3.1038 \pm 0.0006$	$0.097 \pm 0.002$	$0.176 \pm 0.001$
Sn <sub>0.5</sub> Ti <sub>0.5</sub> O <sub>2</sub>	$3.2148 \pm 0.0003$	$0.0549 \pm 0.0006$	$0.1620 \pm 0.0007$
Sn <sub>0.75</sub> Ti <sub>0.25</sub> O <sub>2</sub>	$3.5105 \pm 0.0008$	$0.094 \pm 0.002$	$0.159 \pm 0.002$
SnO <sub>2</sub> -L	$2.822 \pm 0.002$	$0.0224 \pm 0.0003$	$0.0525 \pm 0.0004$

**Table S5.** Derived parameters from PXRD measurements of Sn<sub>x</sub>Ti<sub>1-x</sub>O<sub>2</sub>. Particle size as a function of composition as determined using the Scherrer equation (Equation 3)<sup>8</sup> for the three most intense reflections for each polymorph (101, 200, and 105 for anatase and 110, 101, and 211 for rutile, respectively). Lattice constants,  $a$  and  $c$ , for rutile polymorph samples were determined from the 110 and 101 peaks, respectively. For a-TiO<sub>2</sub>, the 200 and 101 peaks were used to determine  $a$  and  $c$ , respectively. Errors represent uncertainty in fit parameters, propagated as appropriate. For both polymorphs,  $a = b$ .

Sample	Particle Size $d$ (nm)	Lattice $a = b$ (Å)	Constants $c$ (Å)
a-TiO <sub>2</sub>	$22 \pm 2$	$3.7833 \pm 0.0004$	$9.52 \pm 0.01$
r-TiO <sub>2</sub>	$12.6 \pm 0.4$	$4.5924 \pm 0.0006$	$2.9586 \pm 0.0009$
Sn <sub>0.25</sub> Ti <sub>0.75</sub> O <sub>2</sub>	$5.3 \pm 0.5$	$4.626 \pm 0.002$	$3.014 \pm 0.002$
Sn <sub>0.5</sub> Ti <sub>0.5</sub> O <sub>2</sub>	$4.4 \pm 0.8$	$4.676 \pm 0.002$	$3.089 \pm 0.002$
Sn <sub>0.75</sub> Ti <sub>0.25</sub> O <sub>2</sub>	$4.4 \pm 0.5$	$4.691 \pm 0.002$	$3.123 \pm 0.002$
SnO <sub>2</sub> -S	$7 \pm 1$	$4.735 \pm 0.001$	$3.185 \pm 0.001$
SnO <sub>2</sub> -L	$15.8 \pm 0.2$	$4.7375 \pm 0.0004$	$3.1856 \pm 0.0004$

**Table S6.** Dye loadings and film thicknesses of Sn<sub>x</sub>Ti<sub>1-x</sub>O<sub>2</sub>. Dye loadings were determined by UV-Vis measurements in mol cm<sup>-2</sup> as previously described using a modified version of Beer's Law.<sup>6,7</sup> Loadings were determined by the absorbance at 454 nm, where RuP has a molar absorptivity of ~13,400 M<sup>-1</sup> cm<sup>-1</sup>.<sup>6</sup> Film thicknesses were measured by mechanical profilometry, which was then used to convert to volumetric dye loadings in mol cm<sup>-2</sup> μm<sup>-1</sup>.

	Loading (mol cm <sup>-2</sup> ) <sup>a</sup>	Film Thickness (μm) <sup>a</sup>	Loading (mol cm <sup>-2</sup> μm <sup>-1</sup> ) <sup>b</sup>
a-TiO <sub>2</sub>	$(5 \pm 1) \times 10^{-8}$	$5 \pm 1$	$(1.1 \pm 0.3) \times 10^{-8}$
Sn <sub>0.25</sub> Ti <sub>0.75</sub> O <sub>2</sub>	$(1.7 \pm 0.5) \times 10^{-8}$	$0.9 \pm 0.4$	$(1.8 \pm 0.9) \times 10^{-8}$
Sn <sub>0.5</sub> Ti <sub>0.5</sub> O <sub>2</sub>	$(1.3 \pm 0.6) \times 10^{-8}$	$1.1 \pm 0.3$	$(1.2 \pm 0.7) \times 10^{-8}$
Sn <sub>0.75</sub> Ti <sub>0.25</sub> O <sub>2</sub>	$(1.3 \pm 0.2) \times 10^{-8}$	$0.9 \pm 0.2$	$(1.5 \pm 0.5) \times 10^{-8}$
SnO <sub>2</sub> -S	$(1.0 \pm 1.0) \times 10^{-8}$	$0.8 \pm 1.6$	$(1 \pm 3) \times 10^{-8}$
SnO <sub>2</sub> -L	$(1.9 \pm 0.6) \times 10^{-8}$	$4 \pm 1$	$(0.5 \pm 0.2) \times 10^{-8}$

<sup>a</sup> Errors are the standard deviation of the mean.

<sup>b</sup> Errors are propagated from the standard deviations of the loadings and the film thicknesses.

**Table S7.** Powder X-ray diffraction fitting summary for anatase TiO<sub>2</sub>. Errors are the uncertainty in the fit.

Peak Assignment	Location (deg.)	Area	FWHM (deg.)
101	25.312 ± 0.002	2630 ± 30	0.341 ± 0.005
112	36.94 ± 0.04	350 ± 60	0.7 ± 0.1
112	37.840 ± 0.007	780 ± 50	0.35 ± 0.03
112	38.62 ± 0.03	340 ± 50	0.54 ± 0.10
200	48.058 ± 0.005	1400 ± 30	0.42 ± 0.01
105	53.961 ± 0.007	960 ± 40	0.41 ± 0.02
211	55.101 ± 0.008	990 ± 40	0.47 ± 0.02
204	62.742 ± 0.010	840 ± 40	0.48 ± 0.03

**Table S8.** Powder X-ray diffraction fitting summary for rutile TiO<sub>2</sub>. Errors are the uncertainty in the fit.

Peak Assignment	Location (deg.)	Area	FWHM (deg.)
110	27.444 ± 0.003	3770 ± 40	0.674 ± 0.010
101	36.083 ± 0.007	1620 ± 40	0.64 ± 0.02
200	39.19 ± 0.05	730 ± 60	1.3 ± 0.1
111	41.28 ± 0.01	1040 ± 40	0.62 ± 0.03
210	43.96 ± 0.04	800 ± 50	1.2 ± 0.1
211	54.356 ± 0.005	2870 ± 40	0.71 ± 0.01
220	56.62 ± 0.01	990 ± 40	0.64 ± 0.04
002	62.80 ± 0.03	300 ± 70	0.6 ± 0.1
310	64.15 ± 0.04	1400 ± 100	1.48962 0.2

**Table S9.** Powder X-ray diffraction fitting summary for Sn<sub>0.25</sub>Ti<sub>0.75</sub>O<sub>2</sub>. Errors are the uncertainty in the fit.

Peak Assignment	Location (deg.)	Area	FWHM (deg.)
110	27.24 ± 0.01	4720 ± 70	1.53 ± 0.03
101	35.52 ± 0.02	2740 ± 70	1.45 ± 0.05
200	38.9 ± 0.1	400 ± 100	1.2 ± 0.4
111	40.85 ± 0.07	1200 ± 100	1.8 ± 0.2
211	53.82 ± 0.01	5800 ± 100	1.88 ± 0.05
220	55.94 ± 0.05	800 ± 100	1.2 ± 0.2
310	63.67 ± 0.07	1500 ± 100	2.3 ± 0.2

**Table S10.** Powder X-ray diffraction fitting summary for  $\text{Sn}_{0.5}\text{Ti}_{0.5}\text{O}_2$ . Errors are the uncertainty in the fit.

Peak Assignment	Location (deg.)	Area	FWHM (deg.)
110	$26.94 \pm 0.01$	$7010 \pm 90$	$1.80 \pm 0.03$
101	$34.78 \pm 0.02$	$4600 \pm 100$	$1.62 \pm 0.05$
200	$39.10 \pm 0.09$	$1600 \pm 100$	$2.6 \pm 0.3$
211	$52.96 \pm 0.02$	$9500 \pm 300$	$2.49 \pm 0.06$
220	$55.18 \pm 0.08$	$1200 \pm 200$	$1.7 \pm 0.3$
310	$62.91 \pm 0.10$	$300 \pm 70$	$0.9 \pm 0.3$

**Table S11.** Powder X-ray diffraction fitting summary for  $\text{Sn}_{0.75}\text{Ti}_{0.25}\text{O}_2$ . Errors are the uncertainty in the fit.

Peak Assignment	Location (deg.)	Area	FWHM (deg.)
110	$26.86 \pm 0.01$	$7270 \pm 90$	$1.86 \pm 0.03$
101	$34.47 \pm 0.01$	$5300 \pm 100$	$1.69 \pm 0.04$
200	$38.66 \pm 0.06$	$1500 \pm 100$	$2.0 \pm 0.2$
211	$52.63 \pm 0.02$	$8500 \pm 200$	$2.26 \pm 0.05$
220	$55.03 \pm 0.08$	$1100 \pm 200$	$1.7 \pm 0.3$
310	$63.2 \pm 0.1$	$1100 \pm 100$	$2.3 \pm 0.4$

**Table S12.** Powder X-ray diffraction fitting summary for  $\text{SnO}_2\text{-S}$ . Errors are the uncertainty in the fit.

Peak Assignment	Location (deg.)	Area	FWHM (deg.)
110	$26.602 \pm 0.007$	$6030 \pm 70$	$1.22 \pm 0.02$
101	$33.892 \pm 0.006$	$4470 \pm 60$	$0.91 \pm 0.02$
200	$38.07 \pm 0.03$	$2360 \pm 90$	$1.69 \pm 0.09$
211	$51.815 \pm 0.008$	$6510 \pm 90$	$1.35 \pm 0.02$
220	$54.80 \pm 0.03$	$1660 \pm 90$	$1.34 \pm 0.10$
002	$57.97 \pm 0.05$	$450 \pm 60$	$0.8 \pm 0.1$
310	$61.87 \pm 0.04$	$1020 \pm 80$	$1.1 \pm 0.1$
112	$64.78 \pm 0.04$	$760 \pm 90$	$0.7 \pm 0.1$

**Table S13.** Powder X-ray diffraction fitting summary for SnO<sub>2</sub>-L. Errors are the uncertainty in the fit.

Peak Assignment	Location (deg.)	Area	FWHM (deg.)
110	26.587 ± 0.002	4990 ± 40	0.516 ± 0.006
101	33.881 ± 0.002	4830 ± 40	0.518 ± 0.007
200	37.961 ± 0.008	1530 ± 50	0.55 ± 0.03
111	39.02 ± 0.03	240 ± 40	0.35 ± 0.08
211	51.810 ± 0.002	5880 ± 50	0.566 ± 0.006
220	54.768 ± 0.010	1600 ± 50	0.63 ± 0.03
002	57.85 ± 0.03	1070 ± 60	0.93 ± 0.07
310	61.93 ± 0.01	1540 ± 50	0.68 ± 0.03
112	64.77 ± 0.02	1770 ± 90	0.74 ± 0.05

**Table S14.** Fit parameters from high resolution XPS scans of Ti 2p region. Errors are uncertainty in the fit determined using Monte Carlo error analysis in CasaXPS.

Sample	Ti 2p <sub>3/2</sub>			Ti 2p <sub>1/2</sub>		
	Position (eV)	Area <sup>a</sup>	FWHM (eV)	Position (eV)	Area <sup>a</sup>	FWHM (eV)
a-TiO <sub>2</sub>	458.429 ± 0.002	8090 ± 30	0.979 ± 0.004	464.140 ± 0.005	4040 ± 20	1.98 ± 0.01
r-TiO <sub>2</sub>	458.517 ± 0.002	7480 ± 30	0.964 ± 0.004	464.218 ± 0.005	3740 ± 20	1.93 ± 0.01
Sn <sub>0.25</sub> Ti <sub>0.75</sub> O <sub>2</sub>	458.603 ± 0.003	3600 ± 30	1.092 ± 0.008	464.308 ± 0.010	1800 ± 10	2.03 ± 0.02
Sn <sub>0.5</sub> Ti <sub>0.5</sub> O <sub>2</sub>	458.7 ± 0.01	510 ± 20	1.36 ± 0.04	464.44 ± 0.04	253 ± 9	2.24 ± 0.09
Sn <sub>0.75</sub> Ti <sub>0.25</sub> O <sub>2</sub>	458.690 ± 0.010	860 ± 30	1.22 ± 0.03	464.42 ± 0.04	430 ± 10	2.22 ± 0.09
SnO <sub>2</sub> -S	-	-	-	-	-	-
SnO <sub>2</sub> -L	-	-	-	-	-	-

<sup>a</sup> Areas constrained such that the area under the 2p<sub>3/2</sub> peak is twice the area under the 2p<sub>1/2</sub> peak to account for the relative population difference due to spin-orbit splitting.

**Table S15.** Fit parameters from high resolution XPS scans of Sn 3d<sub>5/2</sub> region. Errors are uncertainty in the fit determined using Monte Carlo error analysis in CasaXPS.

Sample	Sn 3d <sub>5/2</sub>			Sn 3d <sub>3/2</sub>		
	Position (eV)	Area <sup>a</sup>	FWHM (eV)	Position (eV)	Area <sup>a</sup>	FWHM (eV)
a-TiO <sub>2</sub>	-	-	-	-	-	-
r-TiO <sub>2</sub>	-	-	-	-	-	-
Sn <sub>0.25</sub> Ti <sub>0.75</sub> O <sub>2</sub>	486.352 ± 0.002	6630 ± 30	1.208 ± 0.005	494.775 ± 0.003	4420 ± 20	1.179 ± 0.006
Sn <sub>0.5</sub> Ti <sub>0.5</sub> O <sub>2</sub>	486.492 ± 0.004	2640 ± 20	1.351 ± 0.008	494.861 ± 0.006	1760 ± 10	1.326 ± 0.010
Sn <sub>0.75</sub> Ti <sub>0.25</sub> O <sub>2</sub>	486.470 ± 0.001	12640 ± 30	1.240 ± 0.003	494.876 ± 0.002	8430 ± 20	1.202 ± 0.004
SnO <sub>2</sub> -S	486.5897 ± 0.0008	42420 ± 40	1.402 ± 0.002	494.998 ± 0.001	28280 ± 30	1.363 ± 0.002
SnO <sub>2</sub> -L	486.4643 ± 0.0008	47450 ± 50	1.357 ± 0.002	494.871 ± 0.001	31630 ± 30	1.319 ± 0.002

<sup>a</sup> Areas constrained such that the area under the 3d<sub>5/2</sub> peak is 1.5 times the area under the 3d<sub>3/2</sub> peak to account for the relative population difference due to spin-orbit splitting.

**Table S16.** Fit parameters from high resolution XPS scans of O 1s region. Errors are uncertainty in the fit determined using Monte Carlo error analysis in CasaXPS.

Sample	O 1s (Metal Oxide, O <sup>2-</sup> )			O 1s (Hydroxide, HO <sup>-</sup> )			O 1s (Water, H <sub>2</sub> O) <sup>a</sup>	
	Position (eV)	Area	FWHM (eV)	Position (eV)	Area	FWHM <sup>a</sup> (eV)	Position (eV)	Area
a-TiO <sub>2</sub>	529.686 ± 0.003	8500 ± 200	1.07 ± 0.01	530.7 ± 0.2	1500 ± 200	2.4 ± 0.2	-	-
r-TiO <sub>2</sub>	529.745 ± 0.003	8290 ± 60	1.051 ± 0.007	531.13 ± 0.05	1080 ± 70	1.56 ± 0.08	533.09 ± 0.03	770 ± 50
Sn <sub>0.25</sub> Ti <sub>0.75</sub> O <sub>2</sub>	529.966 ± 0.008	5280 ± 100	1.15 ± 0.01	531.24 ± 0.09	1100 ± 50	1.51 ± 0.03	532.7 ± 0.02	2980 ± 90
Sn <sub>0.5</sub> Ti <sub>0.5</sub> O <sub>2</sub>	530.29 ± 0.04	1600 ± 200	1.53 ± 0.07	-	-	-	532.41 ± 0.06	3100 ± 300
Sn <sub>0.75</sub> Ti <sub>0.25</sub> O <sub>2</sub>	530.22 ± 0.03	3100 ± 600	1.21 ± 0.10	530.9 ± 0.1	1100 ± 600	1.53 ± 0.02	532.500 ± 0.007	5710 ± 70
SnO <sub>2</sub> -S	530.408 ± 0.006	7100 ± 400	1.12 ± 0.02	531.3 ± 0.1	3900 ± 400	2.06 ± 0.10	-	-
SnO <sub>2</sub> -L	530.329 ± 0.006	8300 ± 400	1.10 ± 0.02	531.2 ± 0.1	4400 ± 500	2.2 ± 0.1	-	-

<sup>a</sup> FWHM of hydroxide (HO<sup>-</sup>) and water (H<sub>2</sub>O) O 1s peaks were constrained to be equal.

**Table S17.** Fit parameters from high resolution XPS scans of C 1s region used for charge correction of other spectra. Values reported are after charge correction has been done. Errors are uncertainty in the fit determined using Monte Carlo error analysis in CasaXPS.

Sample	C 1s (Aliphatic, C-C)			C 1s (Hydroxyl/Ether, C-O) <sup>a,b</sup>	C 1s (Ketone, C=O) <sup>a,b</sup>	C 1s (Ester/Acid, O-C=O) <sup>a,b</sup>
	Position <sup>a</sup> (eV)	Area	FWHM <sup>b</sup> (eV)			
a-TiO <sub>2</sub>	284.80 ± 0.02	680 ± 20	1.27 ± 0.04	190 ± 20	40 ± 10	70 ± 20
r-TiO <sub>2</sub>	284.80 ± 0.01	620 ± 20	1.22 ± 0.03	180 ± 10	22 ± 10	80 ± 10
Sn <sub>0.25</sub> Ti <sub>0.75</sub> O <sub>2</sub>	284.80 ± 0.02	480 ± 20	1.30 ± 0.05	160 ± 10	30 ± 10	60 ± 20
Sn <sub>0.5</sub> Ti <sub>0.5</sub> O <sub>2</sub>	284.80 ± 0.03	210 ± 20	1.46 ± 0.10	19 ± 9	6 ± 9	9 ± 9
Sn <sub>0.75</sub> Ti <sub>0.25</sub> O <sub>2</sub>	284.80 ± 0.05	320 ± 30	1.5 ± 0.1	80 ± 20	20 ± 10	50 ± 20
SnO <sub>2</sub> -S	284.8 ± 0.3	200 ± 100	2.2 ± 0.8	70 ± 30	0 ± 20	70 ± 60
SnO <sub>2</sub> -L	284.80 ± 0.05	240 ± 30	1.2 ± 0.1	140 ± 20	6 ± 10	30 ± 20

<sup>a</sup> Position was charged corrected to the literature value for aliphatic carbons (C-C). Other peak positions for hydroxyl/ether (C-O), ketone (C=O), and ester/acid (O-C=O) were constrained with respect to the aliphatic carbon position ( $E_{C-C}$ ) such that they were  $E_{C-C} + 1.5$  eV,  $E_{C-C} + 3$  eV, and  $E_{C-C} + 4$  eV, respectively.

<sup>b</sup> FWHM values were constrained to be equal across all peaks.

**Table S18.** Peak fitting results for pre-edge features in Ti K-edge XANES spectra. Because the data used were normalized, the error function used to describe the background was fixed with a magnitude of 0.5 (corresponding to unity value).

Assignment	Parameter	a-TiO <sub>2</sub>	r-TiO <sub>2</sub>	Sn <sub>0.25</sub> Ti <sub>0.75</sub> O <sub>2</sub>	Sn <sub>0.5</sub> Ti <sub>0.5</sub> O <sub>2</sub>	Sn <sub>0.75</sub> Ti <sub>0.25</sub> O <sub>2</sub>
Edge	Center (eV)	4981 ± 1	4981.2 ± 0.4	4980.6 ± 0.4	4980.8 ± 0.8	4980.7 ± 1.0
	Width (eV)	2.2 ± 0.3	2.9 ± 0.7	3.2 ± 0.7	2.3 ± 0.4	2.3 ± 0.4
A <sub>1</sub>	Position (eV)	4967.5 ± 0.6	4967 ± 1	4967 ± 1	4967.1 ± 0.9	4967 ± 1
	Area	0.18 ± 0.03	0.18 ± 0.03	0.05 ± 0.01	0.07 ± 0.02	0.07 ± 0.02
	fw hm (eV)	1.6 ± 0.1	1.5 ± 0.3	1.5 ± 0.2	1.6 ± 0.2	1.9 ± 0.3
A <sub>3</sub>	Position (eV)	4970.5 ± 0.8	4969.8 ± 0.2	4969.6 ± 0.3	4969.5 ± 0.3	4969.5 ± 0.3
	Area	0.3 ± 0.1	0.39 ± 0.04	0.39 ± 0.04	0.38 ± 0.04	0.38 ± 0.04
	fw hm (eV)	1.9 ± 0.3	2.21 ± 0.09	2.32 ± 0.10	2.25 ± 0.09	2.04 ± 0.10
B	Position (eV)	4973 ± 4	4973 ± 3	4973 ± 6	4973 ± 5	4973 ± 7
	Area	0.6 ± 0.5	0.6 ± 0.3	0.5 ± 0.7	0.5 ± 0.5	0.5 ± 0.7
	fw hm (eV)	3.4 ± 0.8	3.9 ± 0.3	4.0 ± 0.3	4.1 ± 0.3	4.2 ± 0.4
C	Position (eV)	4978 ± 4	4979 ± 1	4978.2 ± 1.0	4978 ± 3	4978 ± 4
	Area	2 ± 1	2.0 ± 0.6	1 ± 1	2 ± 1	2 ± 1
	fw hm (eV)	4.3 ± 0.2	4.0 ± 0.2	4.2 ± 0.2	4.9 ± 0.1	5.0 ± 0.1
A <sub>2</sub>	Position (eV)	4969 ± 1	-	-	-	-
	Area	0.11 ± 0.02	-	-	-	-
	fw hm (eV)	1.3 ± 0.2	-	-	-	-

**Table S19.** UV-Vis Fit Parameters. Errors are the standard deviation of at least three independent measurements.

Transition	Parameter	a-TiO <sub>2</sub>	Sn <sub>0.25</sub> Ti <sub>0.75</sub> O <sub>2</sub>	Sn <sub>0.5</sub> Ti <sub>0.5</sub> O <sub>2</sub>	Sn <sub>0.75</sub> Ti <sub>0.25</sub> O <sub>2</sub>	SnO <sub>2</sub> -S	SnO <sub>2</sub> -L
T ← S	E <sub>0</sub> (eV)	2.53 ± 0.03	2.49 ± 0.02	2.46 ± 0.04	2.46 ± 0.04	2.407 ± 0.007	2.43 ± 0.01
	FWHM <sub>0</sub> (eV)	0.44 ± 0.04	0.39 ± 0.03	0.35 ± 0.02	0.37 ± 0.04	0.28 ± 0.02	0.23 ± 0.02
	A <sub>0</sub>	0.11 ± 0.02	0.03 ± 0.01	0.016 ± 0.004	0.024 ± 0.004	0.02 ± 0.01	0.019 ± 0.007
0 ← 0	E <sub>1</sub> (eV)	2.695 ± 0.004	2.688 ± 0.003	2.685 ± 0.003	2.683 ± 0.006	2.675 ± 0.005	2.687 ± 0.004
	FWHM <sub>1</sub> (eV) <sup>a</sup>	0.273 ± 0.006	0.276 ± 0.005	0.277 ± 0.004	0.28 ± 0.01	0.288 ± 0.003	0.282 ± 0.005
	A <sub>1</sub>	0.6 ± 0.1	0.18 ± 0.04	0.11 ± 0.04	0.14 ± 0.03	0.2 ± 0.1	0.24 ± 0.09
1 ← 0	E <sub>2</sub> (eV)	2.921 ± 0.003	2.916 ± 0.005	2.914 ± 0.005	2.919 ± 0.007	2.916 ± 0.006	2.920 ± 0.002
	FWHM <sub>2</sub> (eV) <sup>a</sup>	0.273 ± 0.006	0.276 ± 0.005	0.277 ± 0.004	0.28 ± 0.01	0.288 ± 0.003	0.282 ± 0.005
	A <sub>2</sub>	0.56 ± 0.08	0.17 ± 0.04	0.10 ± 0.03	0.13 ± 0.02	0.13 ± 0.10	0.20 ± 0.07
2 ← 0	E <sub>3</sub> (eV)	3.204 ± 0.006	3.20 ± 0.02	3.21 ± 0.02	3.21 ± 0.03	3.24 ± 0.03	3.27 ± 0.02
	FWHM <sub>3</sub> (eV) <sup>a</sup>	0.273 ± 0.006	0.276 ± 0.005	0.277 ± 0.004	0.28 ± 0.01	0.288 ± 0.003	0.282 ± 0.005
	A <sub>3</sub>	0.67 ± 0.05	0.10 ± 0.02	0.06 ± 0.03	0.09 ± 0.02	0.09 ± 0.07	0.15 ± 0.04

<sup>a</sup> <sup>1</sup>MLCT vibronic transitions were constrained to have equal line widths.

**Table S20.** DFT-optimized coordinates and lattice vectors (Å) of  $\text{Sn}_x\text{Ti}_{1-x}\text{O}_2$ .

**a-TiO<sub>2</sub>**

**Lattice vectors:** a = 3.76511874; b = 3.76511874; c = 9.59441947

Atom	x (Å)	y (Å)	z (Å)
O	0.00000000	0.00000000	1.97701192
O	1.88255937	1.88255937	6.77422165
O	0.00000000	1.88255937	4.37561679
O	1.88255937	0.00000000	9.17282652
O	1.88255937	1.88255937	2.82019781
O	0.00000000	0.00000000	7.61740755
O	1.88255937	0.00000000	5.21880268
O	0.00000000	1.88255937	0.42159295
Ti	0.00000000	0.00000000	0.00000000
Ti	1.88255937	1.88255937	4.79720973
Ti	0.00000000	1.88255937	2.39860487
Ti	1.88255937	0.00000000	7.19581460

**r-TiO<sub>2</sub>**

**Lattice vectors:** a = 4.58231625; b = 4.58231625; c = 5.89541529

Atom	x (Å)	y (Å)	z (Å)
O	1.39810559	1.39810559	0.00000000
O	0.89305253	3.68926372	1.47385382
O	3.18421065	3.18421065	0.00000000
O	3.68926372	0.89305253	1.47385382
O	1.39810559	1.39810559	2.94770764
O	0.89305253	3.68926372	4.42156147
O	3.18421065	3.18421065	2.94770764
O	3.68926372	0.89305253	4.42156147
Ti	0.00000000	0.00000000	0.00000000
Ti	2.29115812	2.29115812	1.47385382
Ti	0.00000000	0.00000000	2.94770764
Ti	2.29115812	2.29115812	4.42156147

**Sn<sub>0.25</sub>Ti<sub>0.75</sub>O<sub>2</sub>**

**Lattice vectors:** a = 4.62679222; b = 4.62679222; c = 6.02665254

Atom	x (Å)	y (Å)	z (Å)
O	1.41498443	1.41498443	0.00000000
O	0.92430150	3.70375747	1.43490370
O	3.21307454	3.21307454	0.00000000
O	3.70375747	0.92430150	1.43490370
O	1.44769005	1.44769005	3.01332627
O	0.92430150	3.70375747	4.59174883
O	3.18036892	3.18036892	3.01332627
O	3.70375747	0.92430150	4.59174883
Sn	0.00000000	0.00000000	3.01332627
Ti	2.31402948	2.31402948	1.47679023
Ti	0.00000000	0.00000000	0.00000000
Ti	2.31402948	2.31402948	4.54986231

**Sn<sub>0.5</sub>Ti<sub>0.5</sub>O<sub>2</sub>**

**Lattice vectors:** a = 4.66285330; b = 4.66285330; c = 6.17400232

Atom	x (Å)	y (Å)	z (Å)
O	1.40320607	1.40320607	6.09631858
O	0.88988867	3.77296463	1.47737780
O	3.25964723	3.25964723	6.09631858
O	3.77296463	0.88988867	1.47737780
O	1.44153798	1.44153798	3.15312395
O	0.92822058	3.73463272	4.70818548
O	3.22131532	3.22131532	3.15312395
O	3.73463272	0.92822058	4.70818548
Sn	0.00000000	0.00000000	3.10636144
Sn	2.33142665	2.33142665	1.52414030
Ti	0.00000000	0.00000000	6.12606114
Ti	2.33142665	2.33142665	4.67844292

## **Sn<sub>0.75</sub>Ti<sub>0.25</sub>O<sub>2</sub>**

**Lattice vectors:** a = 4.71198203; b = 4.71198203; c = 6.27949859

Atom	x (Å)	y (Å)	z (Å)
O	1.46053526	1.46053526	6.21291140
O	0.91920095	3.79849073	1.56987465
O	3.25715642	3.25715642	6.21291140
O	3.79849073	0.91920095	1.56987465
O	1.46053526	1.46053526	3.20633649
O	0.96132429	3.75636738	4.70962394
O	3.25715642	3.25715642	3.20633649
O	3.75636738	0.96132429	4.70962394
Sn	0.00000000	0.00000000	3.16666376
Sn	2.35884584	2.35884584	1.56987465
Sn	0.00000000	0.00000000	6.25258413
Ti	2.35884584	2.35884584	4.70962394

## **SnO<sub>2</sub>**

**Lattice vectors:** a = 4.75964688; b = 4.75964688; c = 6.38361102

Atom	x (Å)	y (Å)	z (Å)
O	1.45677288	1.45677288	0.00000000
O	0.92305056	3.83659632	1.59590275
O	3.30287400	3.30287400	0.00000000
O	3.83659632	0.92305056	1.59590275
O	1.45677288	1.45677288	3.19180551
O	0.92305056	3.83659632	4.78770826
O	3.30287400	3.30287400	3.19180551
O	3.83659632	0.92305056	4.78770826
Sn	0.00000000	0.00000000	0.00000000
Sn	2.37982344	2.37982344	1.59590275
Sn	0.00000000	0.00000000	3.19180551
Sn	2.37982344	2.37982344	4.78770826

## References

1. Trotochaud, L.; Boettcher, S. W., Synthesis of Rutile-Phase  $\text{Sn}_x\text{Ti}_{1-x}\text{O}_2$  Solid-Solution and  $(\text{SnO}_2)_x/(\text{TiO}_2)_{1-x}$  Core/Shell Nanoparticles with Tunable Lattice Constants and Controlled Morphologies. *Chem. Mater.* **2011**, *23*, 4920-4930.
2. Meites, L., *Handbook of Analytical Chemistry*. McGraw Hill Book Co., Inc.: New York, 1963.
3. Naumkin, A. V.; Kraut-Vass, A.; Gaarenstroom, S. W.; Powell, C. J., NIST X-ray Photoelectron Spectroscopy Database. In *NIST Standard Reference Database Number 20*, 2000 ed.; National Institute of Standards and Technology: Gaithersburg, MD 20899, 2000.
4. Ramamoorthy, M.; Vanderbilt, D.; King-Smith, R. D., First-Principles Calculations of the Energetics of Stoichiometric  $\text{TiO}_2$  Surfaces. *Phys. Rev. B* **1994**, *49*, 16721-16727.
5. Ravel, B.; Newville, M., ATHENA, ARTEMIS, HEPHAESTUS: Data Analysis for X-ray Absorption Spectroscopy Using IFEFFIT. *J. Synchrotron. Radiat.* **2005**, *12*, 537-541.
6. Hanson, K.; Brennaman, M. K.; Ito, A.; Luo, H.; Song, W.; Parker, K. A.; Ghosh, R.; Norris, M. R.; Glasson, C. R. K.; Concepcion, J. J.; Lopez, R.; Meyer, T. J., Structure–Property Relationships in Phosphonate-Derivatized,  $\text{Ru}^{\text{II}}$  Polypyridyl Dyes on Metal Oxide Surfaces in an Aqueous Environment. *J. Phys. Chem. C* **2012**, *116*, 14837-14847.
7. Jiang, J.; Spies, J. A.; Swierk, J. R.; Matula, A. J.; Regan, K. P.; Romano, N.; Brennan, B. J.; Crabtree, R. H.; Batista, V. S.; Schmuttenmaer, C. A.; Brudvig, G. W., Direct Interfacial Electron Transfer from High-Potential Porphyrins into Semiconductor Surfaces: A Comparison of Linkers and Anchoring Groups. *J. Phys. Chem. C* **2018**, *122*, 13529-13539.
8. Scherrer, P., Bestimmung der Größe und der Inneren Struktur von Kolloideilchen Mittels Röntgenstrahlen. *Nachr. Ges. Wiss. Goettingen, Math.-Phys. Kl.* **1918**, *2*, 98-100.